Aspects of Sensor Networks

Matthias Weiß

Fraunhofer-Institut für Hochfrequenzphysik und Radartechnik FHR
Passive Sensoren und Klassifizierung
Neuenahrer Straße 20, 53343 Wachtberg, Germany

E-Mail: matthias.weiss@fhr.fraunhofer.de

Abstract

In many surveillance and tracking systems multi-sensor configurations are used to provide a greater depth of information on the target and likewise to increase the robustness of the sensor network to survive individual sensor failure.
This lecture investigates several aspects of sensor networks and illustrates various properties of distributed networks composed of identical sensors.

1 Introduction

Sensor networks are very attractive for reconnaissance and surveillance applications as they provide more information from the same target, which helps to identify, classify, and track it. Furthermore, sensor networks possess a higher probability to survive if individual sensors fail. Looking at a sensor network and its operation these can be divided into two main categories:

- mono-type and

[0]Weiß, M. (2010) Aspects of Sensor Networks. In *Multisensor Fusion: Advanced Methodologies and Applications* (pp. 10-1 — 10-15). Educational Notes RTO-EN-SET-157, Paper 10. Neuilly-sur-Seine, France: RTO. Available from: http://www.rto.nato.int.abstracts.aps.

Report Documentation Page

Form Approved
OMB No. 0704-0188

1. REPORT DATE	2. REPORT TYPE	3. DATES COVERED
MAY 2010	**N/A**	**-**

4. TITLE AND SUBTITLE	5a. CONTRACT NUMBER
Aspects of Sensor Networks	5b. GRANT NUMBER
	5c. PROGRAM ELEMENT NUMBER
6. AUTHOR(S)	5d. PROJECT NUMBER
	5e. TASK NUMBER
	5f. WORK UNIT NUMBER
7. PERFORMING ORGANIZATION NAME(S) AND ADDRESS(ES) **Fraunhofer-Institut f¨ur Hochfrequenzphysik und Radartechnik FHR Passive Sensoren und Klassifizierung Neuenahrer Straße 20, 53343 Wachtberg, Germany**	8. PERFORMING ORGANIZATION REPORT NUMBER
9. SPONSORING/MONITORING AGENCY NAME(S) AND ADDRESS(ES)	10. SPONSOR/MONITOR'S ACRONYM(S)
	11. SPONSOR/MONITOR'S REPORT NUMBER(S)

12. DISTRIBUTION/AVAILABILITY STATEMENT
Approved for public release, distribution unlimited

13. SUPPLEMENTARY NOTES
See also ADA564550. Multisensor Fusion: Advanced Methodology and Applications (Fusion multicapteur : Methodologie evoluee et Applications). RTO-EN-SET-157(2010)

14. ABSTRACT
In many surveillance and tracking systems multi-sensor configurations are used to provide a greater depth of information on the target and likewise to increase the robustness of the sensor network to survive individual sensor failure. This lecture investigates several aspects of sensor networks and illustrates various properties of distributed networks composed of identical sensors.

15. SUBJECT TERMS

16. SECURITY CLASSIFICATION OF:			17. LIMITATION OF ABSTRACT	18. NUMBER OF PAGES	19a. NAME OF RESPONSIBLE PERSON
a. REPORT	b. ABSTRACT	c. THIS PAGE			
unclassified	**unclassified**	**unclassified**	**SAR**	**16**	

- multi-type sensor networks.

Networks composed of different sensor types allow to determine various characteristics of the same target and therefore improve the classification and identification task, but not necessarily the target localization accuracy.
Depending on the arrangement of the sensors in the network a further classification can be introduced as

- colocated network and
- distributed sensor network.

Any combination of these first categories is possible, but generally different sensors are located nearby to observe the same area. An example of a colocated mono-type sensor network is the virtual linear array antenna, composed of several transmit and receive antennas arranged along a straight line [1]. For such a configuration the signal processing will be performed by a central processing unit, which ensures that the network operates coherently. The common architecture of distributed multi-sensor networks is to install a preprocessing at each receiver node and transfer the results over a high-speed communication link to a further processing stage for data fusion. Depending on the signal bandwidth and complexity of the distributed network also a central processing solution may be feasible, depending on the communication link between the nodes and the central unit [2].
The advantage of a distributed mono-type sensor network is the possibility of bi-/multistatic operation. That implies, a receiver node is able to receive echoes from the target illuminated from different transmit nodes. Furthermore, spatially distributed mono-type sensor networks offer more degrees of freedom than a system with one sensor. These multiple-input multiple-output (MIMO) networks support flexible time-energy management modes, exhibit higher angular resolution, show an improved parameter estimation, and facilitate high resolution target localization accuracy with an improved detectability by exploiting target echo (RCS) diversity [3]. An optimal MIMO network comprises multiple transmitters and multiple receivers to pick-up the reflected signal. Radar systems with their all-day, all weather ability are promising sensors for MIMO networks for surveillance applications in defence and civilian categories. On the contrary, if a networks is composed of different sensor types each node can only operate in a monostatic configuration.

A MIMO network can be split up into two principal categories of operation based on transmitter usage [10]:

- spatial multiplexing and
- space time transmit diversity

In the *spatial multiplexing* case, each transmit node in the network has an unique orthogonal coded signal, which is transmitted in the same frequency channel. If these electromagnetic waves arrive at the receive node, the receiver can separate these signals by matched filters, creating as many parallel channels as transmit nodes exists. Spatial multiplexing is a very powerful technique for increasing MIMO network capacity and can be used with or without transmit channel knowledge.
In contrast to the spatial multiplexing case all transmit nodes share the same waveform and frequency channel in the *space time transmit diversity* case. Due to this, always only one transmitter is active. After the transmitted and reflected signal has arrived at all receive nodes the next transmitter will emit a signal. As the time t_0 of each firing is known the receivers can assign the received signal to the corresponding transmitter [3].

The following sections of this lecture will focus on MIMO radar networks, representative for all other mono-type sensor networks, and will discuss some essential design aspects to obtain the optimal performance for a given configuration.

2 Synchronisation

In a sensor network synchronisation between all nodes is essential for the performance of the system and can be parted in three areas: timing, frequency, and phase. Timing synchronisation is needed between transmit and receive nodes for range measurement and typically an accuracy in the order of a fraction of the transmitted compressed pulse is required $\tau = 1/B$, where B is the signal bandwidth [4].

If the network nodes are not too far separated from each other synchronising the stable local oscillators can be achieved by connecting them together by cable, fibre or direct communication link. If there is no direct line of sight available, time synchronisation can also be achieved via a scattering signal (clutter) or even a scattering of the troposphere. A prerequisite is that the scattering volume is detected by transmit and receive antenna lobes. This method is not suitable to stabilize two local oscillators via a phase-locked loop as one can aspect a large variation (jitter) in the time base if the scattering body moves, for instance by gusts of wind. Commercially available are a range of various qualities of stable oscillators ranging from a simple quartz oscillators, temperature controlled quartz with single or double ovens for stable operating temperature, to more expensive atomic clocks such as rubidium or caesium oscillators.

Due to the inherent aging and instability, the local references must be continuously re-synchronised on a time interval, which depends on the required stability and coherence in

the network. The stability directly influences the coherent integration time in the sensor network. Another important aspect of reference oscillators in a distributed MIMO radar network is their phase noise characteristic. While in a single sensor system and its monostatic operation the received echo has some correlation with the transmitted signal, even at great distances, such a correlation does not exist in a MIMO network with several independent reference clocks.

Phase noise is a representation of random fluctuations in the phase of a waveform and is specified in frequency domain for a given frequency offset from the carrier e.g. $\mathcal{L} = 110\,\mathrm{dBc}$ at $10\,\mathrm{Hz}$ and/or in time domain by the two-point variance (Allan variance) for a set of time intervals. Particularly for detecting slow moving targets which introduce a small Doppler shift a low phase noise close to the carrier is very important for the Doppler processing. Attention has to be paid when the system is mounted on a vibrating platform, such as an airplane, as oscillators are sensitive against accelerations and phase noise will degrade [5]. A comparison between some standard oscillators and their single sideband noise ($\mathcal{L}$ in [dBc/Hz]) is shown in table 1.

Table 1: Comparison of various stable oscillators at 10 MHz

	TCXO	OCXO	OCXO(BVA)	MCXO	Rubidium	Cesium	GPS
temperature stability	$1{\cdot}10^{-6}$	$2{\cdot}10^{-8}$	$1{\cdot}10^{-10}$	$2{\cdot}10^{-8}$	$2{\cdot}10^{-8}$	$2{\cdot}10^{-8}$	—
drift per day	$1{\cdot}10^{-8}$	$1{\cdot}10^{-10}$	$5{\cdot}10^{-12}$	$5{\cdot}10^{-11}$	$5{\cdot}10^{-13}$	$3{\cdot}10^{-14}$	$3{\cdot}10^{-14}$
short-time stability $\sigma_y(\tau)$	$1{\cdot}10^{-9}$	$1{\cdot}10^{-12}$	$5{\cdot}10^{-13}$	$1{\cdot}10^{-10}$	$5{\cdot}10^{-12}$	—	—
1s	$1{\cdot}10^{-10}$	$1{\cdot}10^{-11}$	$1{\cdot}10^{-12}$	$2{\cdot}10^{-8}$	$1{\cdot}10^{-11}$	$6{\cdot}10^{-11}$	—
100 s	$3{\cdot}10^{-10}$	$1{\cdot}10^{-11}$	$1{\cdot}10^{-12}$	$2{\cdot}10^{-8}$	$1{\cdot}10^{-13}$	$6{\cdot}10^{-12}$	—
1 day	$1{\cdot}10^{-12}$	$3{\cdot}10^{-12}$	$3{\cdot}10^{-12}$	$5{\cdot}10^{-10}$	$1{\cdot}10^{-13}$	$6{\cdot}10^{-12}$	—
$\mathcal{L}$ @ 1Hz	-50	-100	-122	-115	-80	-85	—
$\mathcal{L}$ @ 10Hz	-80	-130	-137	-135	-98	-125	—
$\mathcal{L}$ @ 100Hz	-110	-140	-145	-145	-137	-135	—
$\mathcal{L}$ @ 1kHz	-120	-145	-156	-150	-150	-140	—

If no direct synchronisation is possible, as the baseline is too large for any cable or fibre, or no line-of-sight exists, the local oscillators of each network node can be indirectly synchronised by use of a Global Navigation Satellite System (GNSS) which provides a highly stable time reference. This time reference, the 1 Pulse-Per-Second (PPS) signal, can be used to discipline the local oscillator. The uncertainty in time of a 1PPS is in the order of $100\,\mathrm{ns}$

or less. If two GNSS receivers are receiving navigation signals from the same satellites, which is possible up to a distance of $8000\,\mathrm{km}$ between them, an accuracy of $5...20\,\mathrm{ns}$ can be achieved, even if the selective available (SA) signal is activated. Only the location of the GNSS receiver must known precisely ($\leq 1\,\mathrm{m}$). This can be easily obtained by an averaging of the calculated position from the GNSS data over several days. Figure 1 shows the phase difference between two temperature controlled crystal oscillators which were disciplined by different GPS receivers and their PPS signal. The standard deviation of the 1PPS signal was $50\,\mathrm{ns}$ for each GPS receiver. Each GPS receiver has been set into the mobile mode, which means that the receiver has to solve the full set of equations to determine the position and time for each GPS epoch. Therefore, a lower variance can be expected if both GPS units works in the *stationary mode*, where the location of the GPS receiver is known and only the time has to be determined from the GPS signals [6].

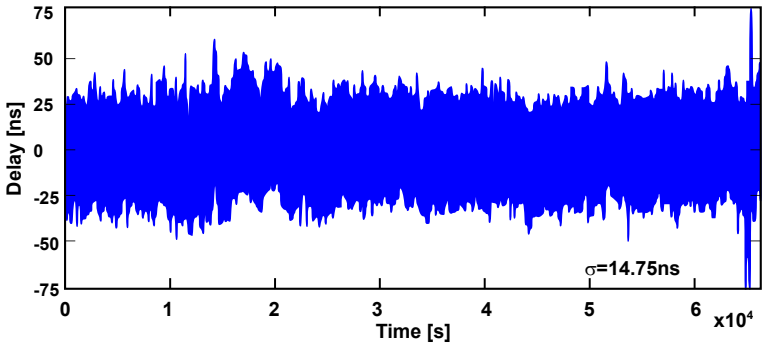

Figure 1: Measured phase difference between two GPS disciplined TCXO at 10 MHz

In this configuration the local oscillator determines the short time stability, while the long time stability is determined by the stability of the GPS system. As long as the receiver is locked to the GPS, the long time stability is ensured. In the case of GPS jamming or receiver unlock, the stability of the local oscillator unit will determine the drift due to aging and temperature changes etc.

2.1 Phase synchronisation

For Doppler or MTI processing phase coherence between transmit and receive nodes has to be established, which allows to reject clutter or chaff. The phase coherence can be obtained in the same ways as time coherence. Using indirect phase synchronisation, which is the best solution, involves high-precision oscillators at the network nodes that are re-synchronised via the 1PPS provided by the GNSS receiver. Over the whole coherent integration time τ_k

the phase stability has to be guaranteed and equal to $\Delta\phi \,/\, 2\pi f \tau_k$ [4]. For a ground based bistatic radar with a center frequency of $3\,\mathrm{GHz}$, a maximum phase deviation of $\Delta\phi = 4^\circ = 0,07\,\mathrm{mrad}$ and a coherent integration time of $\Delta\tau_k = 1\,\mathrm{ms}$ the required oscillators stability is $3.7 \cdot 10^{-12}$. This requirement can be fulfilled with a temperature-controlled crystal oscillator, as can be taken from table 1.

Likewise the phase synchronisation can be achieved by a direct signal, if a line-of-sight exists. If the synchronisation takes place along each transmit pulse a phase stability can be reached of $\Delta\phi \,/\, 2\pi f \Delta T_{rt}$, with ΔT_{rt} denoting the travelling time difference between transmitter-target-receiver and the direct signal transmitter-receiver. $\Delta\phi$ is the allowed phase difference in *rad*. If an accuracy of $\Delta\phi = 4^\circ = 0,07\,\mathrm{rad}$ is requested at a center frequency of $f = 10\,\mathrm{GHz}$ and the time difference $\Delta T_{rt} = 1\,\mathrm{ms}$ ($\Delta r_{rt} = 300\,\mathrm{km}$) the oscillator must have a stability of 10^{-9}, which can easily be achieved by a simple quartz oscillator.

3 Ambiguity function

An important tool to evaluate radar or sonar signal processing performance in terms of range and Doppler resolution as well as clutter rejection is the ambiguity function. The concept of ambiguity function was first introduced by *Woodward* [7]. It is a two dimensional function of time delay and Doppler frequency $\chi(\tau, f_D)$) showing the absolute envelope of the output of the receiver matched filter when the input to the filter is a Doppler shifted version of the original transmitted signal. The ambiguity function is determined only by the properties of the received pulse and the matched filter, which represents the transmitted pulse, and not any specific target scenario. Many definitions of the ambiguity function exist. Several focus on narrowband signals and other are applicable to describe the propagation delay and Doppler relationship of wideband signals. For a complex baseband signal $s(t)$, which fulfils the narrowband condition $2vBT/c \ll 1$, where v is the target velocity, B is the signal bandwidth, T is the pulse duration, and c is the speed of propagation, the narrowband ambiguity function is given by [7]:

$$\left|\chi(\tau, f_D)\right|^2 \;=\; \left| \int_{-\infty}^{\infty} s(t) \cdot s^*(t-\tau) \cdot e^{j2\pi f_D t}\, dt \right|^2 \qquad (1)$$

where * denotes the complex conjugate and f_D the Doppler shift in frequency. An important assumption for the target is that its scattering properties do not change over the pulse duration and with the look angles and that is only slowly manoeuvring.

The monostatic ambiguity function was developed for a single colocated transmit/receive pair and is fairly well developed and understood [8]. It has been shown that the ambiguity

function arises from the detection and parameter estimation problems joined with a slowly fluctuating point target being observed in additive white Gaussian noise.

For bistatic geometry the simple relationship between time delay and range and between target velocity and Doppler shift is no longer valid and therefore Tsao et al. [9] have developed the bistatic ambiguity function. It is shown that the bistatic geometry has a strong influence on the ambiguity function $\chi(\tau, f_D)$, which can be written as:

$$\begin{aligned}\left|\chi(R_{R_H}, R_{R_A}, V_H, V_A, \theta_R, L)\right|^2 \;=\; \Big| \int_{-\infty}^{\infty} & s(t-\tau_a(R_{R_A}, \theta_R, L)) \cdot s^*(t-\tau_H(R_{R_H}, \theta_R, L)) \\ & \cdot \exp\{-j(\omega_{DH}(R_{R_H}, V_H, \theta_R, L) \\ & -\omega_{DA}(R_{R_A}, V_A, \theta_R, L))\, t\}\, dt\Big|^2 \end{aligned} \tag{2}$$

in which R_R and R_T are the ranges from the target to the receiver respectively to the transmitter, V is the target radial velocity, θ_R is the angle of the target measured from the receiver, L is the bistatic baseline, τ is the transmitter-target-receiver delay time, and the subscription H and A denote the hypothesized and actual values.

The important difference between the monostatic (1) and bistatic ambiguity function (2) is that the geometrical layout of the transmitter, receiver and target are now taken into account. This can have a significant effect on the form of the ambiguity function and the resulting range and Doppler resolutions. For the following examples a pulse is considered with a complex envelope described by a simple Gaussian shape:

$$s(t) \;=\; \left(\frac{1}{\pi T^2}\right)^{1/4} \exp\left(-\frac{t^2}{2\,T^2}\right) \qquad -\infty \le t \le \infty \quad , \tag{3}$$

with T the pulse duration. The monostatic ambiguity function for such a pulse is shown in Fig. 2. The following parameters where assumed for the simulations of the ambiguity function: pulse duration $T = 120\,\mu$s, time delay $\tau = 400\,\mu$s, and center frequency $f_c = 50\,$MHz. All figures show the considered geometry (left subplot), the normalized ambiguity function as a function of velocity and target range from the receiver (center plot), and an equal-height contour plot (right subplot). As the linear relationship between delay and range, and Doppler shift and radial velocity is no more valid in the bistatic case the ambiguity function is plotted with respect to range and velocity. For the monostatic case these plots are identical. However, when targets are near or even crossing the bistatic baseline the bistatic ambiguity function changes dramatically, as shown in Fig. 3 and Fig. 4. Especially if the target crosses the baseline perpendicularly no resolution in range or Doppler can be obtained, hence, the bistatic ambiguity function in this area is zero, regardless of the position of the target on the baseline and the velocity.

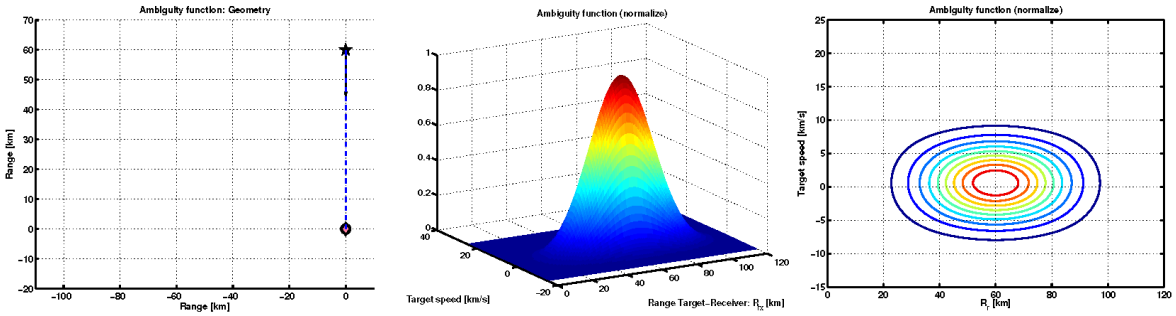

Figure 2: Monostatic ambiguity function plot of Gaussian pulse: left figure shows the geometry, center figure a three dimensional plot, and on the right side a contour plot is shown.

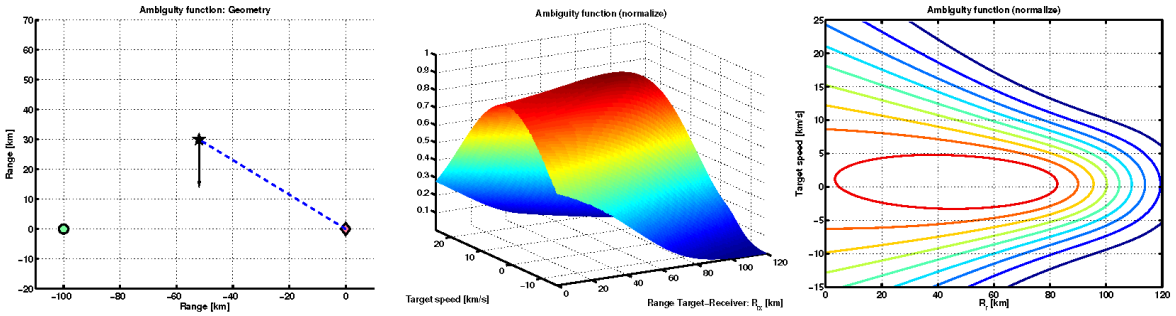

Figure 3: Bistatic ambiguity function plot of Gaussian pulse: left figure shows the geometry, center figure a 3 dimensional plot in the range-velocity plane, and on the right side a contour plot is shown.

For a MIMO radar network, which can be seen as a composition of several bistatic transmit receive pairs, the ambiguity function is formulated based on the bistatic ambiguity function. It is assumed that the network is composed of M transmitters and N receivers. In that case the network shows MN bistatic pairs. To simplify the derivation of the multistatic ambiguity function the same assumptions are made as for the bistatic ambiguity function. Furthermore, it is assumed that the network is coherent. This implies that the echoes arriving at different time instances can be processed jointly. Similar to the bistatic radar ambiguity analysis, the multistatic radar ambiguity function is developed by the following three steps [10]:

(i) For each transmitter-receiver-pair the bistatic ambiguity (2) function is calculated
(ii) Calculating a weighting factor according to received signal intensity

$$P_{ij} = \frac{P_i\, G_i\, G_j\, \lambda^2 \sigma_B}{(4\pi)^3\, R^2_{tx_i \to t}\, R^2_{t \to rx_j}} \tag{4}$$

$$w_{ij} = \frac{P_{ij}}{Max(P_{ij})} \tag{5}$$

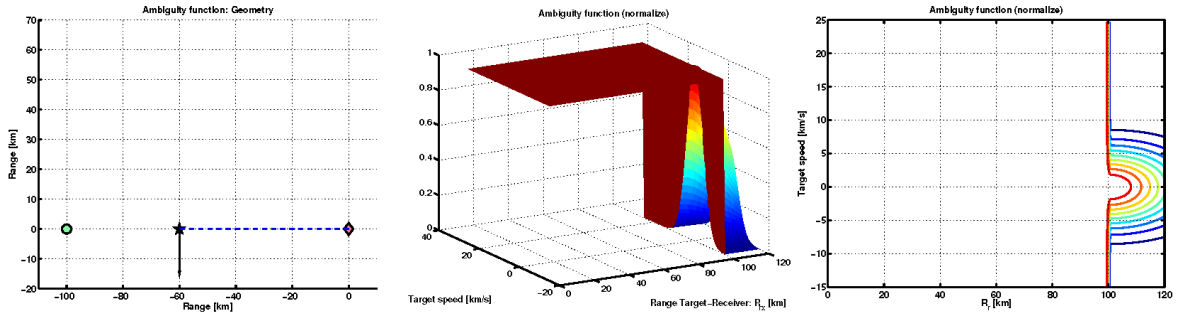

Figure 4: Bistatic ambiguity function plot of Gaussian pulse: left figure shows the geometry, center figure a 3 dimensional plot in the range-velocity plane, and on the right side a contour plot is shown.

(iii) To formulate multistatic radar ambiguity function using the results from previous calculations:

$$\chi_{multi} = \left| \frac{1}{M^2 N^2} \sum_{i=1}^{M} \sum_{j=1}^{N} w_{ij} \chi_{ij} \right|^2 \tag{6}$$

A multistatic radar model has been developed for a comprehensive understanding of multistatic radar ambiguity performance. It is assumed that the fixed transmitters and receivers are located in one plane and the target is moving in another plane, which is parallel to the transmitter-receiver plane. This tool is very useful to evaluate the performance of a given multistatic network.

4 Target localisation

Due to their improved target parameter estimation capability distributed MIMO radar networks are very attractive for system designers. In particular their improved angular resolution capability and ability to separate multiple targets [12], [13], to improve parameter identification [14], and to improve radar performance by exploiting radar cross section (RCS) diversity is very attractive for surveillance applications [15]. Likewise MIMO radar networks can handle slow moving targets by exploiting Doppler estimates from multiple directions [16] and feature a highly accurate estimation of target position [17], [18].

The estimation of target localisation in a MIMO radar network can be performed in a coherent or non-coherent way based on best linear unbiased estimator (BLUE).

The distributed MIMO radar network consists of M transmit and N receive nodes, which are located in the two-dimensional plane (x, y). The transmitters are located at $T_k = (x_{tk}, y_{tk})$, with $k = 1, ..., M$, and the coordinates of the receivers are $R_l = (x_{rl}, y_{rl})$. Each transmitter emits an orthogonal waveform, with a lowpass equivalent $s_k(t)$, $k = 1, ..., M$. All waveforms are narrowband signals fulfilling the assumption of $(B/f_c)^2 \ll 1$. The target at the position $X = (x, y)$ has a complex radar cross section ζ, which does not change over the aspect angle, and introduces a time delay τ_{lk} for each received signal. Taking into account these assumptions the equivalent lowpass received signal at receiver l can be described by [20]:

$$r_l(t) \;=\; \sum_{k=1}^{M} \zeta s_k(t - \tau_{lk}) e^{-j2\pi f_c \tau_{lk}} \;+\; n_l(t) \tag{7}$$

with $n_l(t)$ the complex Gaussian white noise. The target location can be computed by the time difference of arrival (TDOA) of the received signal to more than two receivers. In Eq. (7) the time delays τ_{lk} , which are determined by the location of the target, the transmitters, and receivers, are given by the following relation:

$$\tau_{lk} \;=\; \frac{1}{c}\Big[\sqrt{(x_{tk} - x)^2 + (y_{tk} - y)^2} \;+\; \sqrt{(x_{rl} - x)^2 + (y_{rl} - y)^2}\Big] \tag{8}$$

The target localisation processing uses the well-established multilateration principle and can be performed coherently or non-coherently. In the non-coherent case each receiver node in the MIMO network has only timing information on all emitted waveforms, but no knowledge of the phase. Hence, as no phase information is available for non-coherent localisation the received signal in Eq. (7) simplifies to:

$$r_l(t) \;=\; \sum_{k=1}^{M} \alpha_{lk} s_k(t - \tau_{lk}) \;+\; n_l(t) \tag{9}$$

where α_{lk} are unknown complex amplitudes effected by the targets radar cross section and the phase offset between transmitter and receiver.

The goal of the multi radar network is to estimate the target position $X = (x, y)$. This can be achieved by formulating the maximum likelihood estimate (MLE) using the equation sets given by Eq. (7). Another way to determine the target location is to estimate first the time delays τ_{lk} from the equations formed by Eq. (8) and to compute in a second step the position by employing multilateration principles.

Another approach proposed by Godrich et al. [11] uses a linear model in estimating the time delays τ_{lk} given by the output of the matched filter to the transmitted signals $s_k(t)$. For a

fully coherently operating radar network, each node has global time and phase information, and the estimation is given by:

$$\chi_{c,lk}(\tau_{lk}) \quad = \quad \zeta^* \int r_l(t) \cdot s_k^*(t-\tau_{lk})\, e^{j2\pi f_c \tau_{lk}}\, \mathrm{d}t \quad . \tag{10}$$

The only unknown parameter which has to be estimated as well is the complex radar cross section ζ, which introduces an unknown phase shift. The integration has to be taken over the pulse duration of the transmitted signal $s_k(t)$.

For a non-coherent network, where no phase information is available, Eq. (10) simplifies to:

$$\chi_{nc,lk}(\tau_{lk}) \quad = \quad \alpha_{lk}^* \int r_l(t) \cdot s_k^*(t-\tau_{lk})\, \mathrm{d}t \tag{11}$$

The unknown complex amplitudes α_{lk} have no impact on determining the time delays as they are independent from each other.

4.1 Position dilution of precision (PDOP)

A good tool for visualizing locating accuracy for a given multistatic radar network layout is the PDOP mapping, which was originated with launching the Loran-C navigation system and came into much wider usage with GPS [21]-[24]. The dilution of precision can be interpreted as an expression which describes the impact of the positions of the transmit and receive nodes of a sensor network on the relationship between the estimated time delay and the localization errors. Hence, plots of PDOP give a deep insight in the achievable localization accuracy for a given set multisite radar network configuration.

For each measurement error a corresponding dilution of precision can be defined. For the two dimensional case, where $X = (x, y)$, it is:

$$PDOP \quad = \quad \frac{\sqrt{\sigma_x^2 + \sigma_y^2}}{\sigma_R} \tag{12}$$

$$TDOP \quad = \quad \frac{\sqrt{\sigma_t^2}}{\sigma_R} \tag{13}$$

$$GDOP \quad = \quad \sqrt{PDOP^2 + TDOP^2} \tag{14}$$

where σ_R^2 is the standard deviation of the range estimation, defined by standard deviation of the time delays $c^2\sigma_t^2$, σ_x^2 and σ_y^2 are the variances of the localization on the x and y axis, respectively. Furthermore we define two more DOP's, one for the horizontal x-axis $HxDOP = \sqrt{\sigma_x^2}/\sigma_R$ and one for the horizontal y-axis $HyDOP = \sqrt{\sigma_y^2}/\sigma_R$.

In Fig. 5 contour maps of the PDOP for a non-coherent (left plot) and coherent (plot on the right side) radar network are shown. The multistatic radar network consists of 4 transmitters and receivers, equally placed on a circle. Each transmitter emits orthogonal waveforms and the receivers estimate the time delay. From these estimated time delays the target position is determined by solving Eq. (10) or for the non-coherent case Eq. (11). The green and red

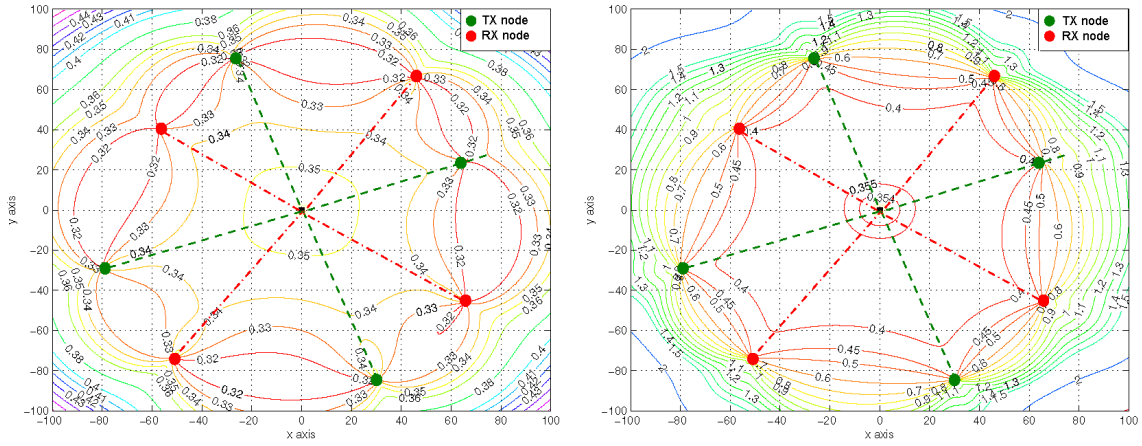

Figure 5: PDOP contour plot with 4 transmitters and 4 receivers radar network symmetrical placed. Left figure shows the accuracy of non-coherent and right figure the coherent processing case, respectively. (©IEEE 2009, from [20])

dots in the PDOP maps represent the transmitters and receivers of the radar network. For the coherent case a target located inside the network circle shows lower PDOP values than targets located outside. In comparison to the non-coherent case the accuracy does not change much for target inside the observation circle and the lowest PDOP value is obtained at the center. Outside the radar network the localization errors rises dramatically for the coherent case. If the network operates non-coherently the best PDOP is between each transmit-receive pair and degrades smoothly in both directions from the baseline.

In the second example the transmitters and receivers form nearly a semicircle, as depicted in Fig. 6 by red and green dots. Clearly visible is the degradation of the accuracy of measurements for the coherent case, in comparison to the symmetrical configuration. These examples show that high localisation accuracy can be obtained if the target is encircled by the nodes of the radar network. Hence, the location of transmitters and receivers has to be chosen carefully to obtain the demanded accuracy. In contrast to the coherent case the non-coherent processing does not show significant degradation in comparison to a symmetrical setup.

Maps of PDOP represent a very useful tool for showing the accuracy which can be ob-

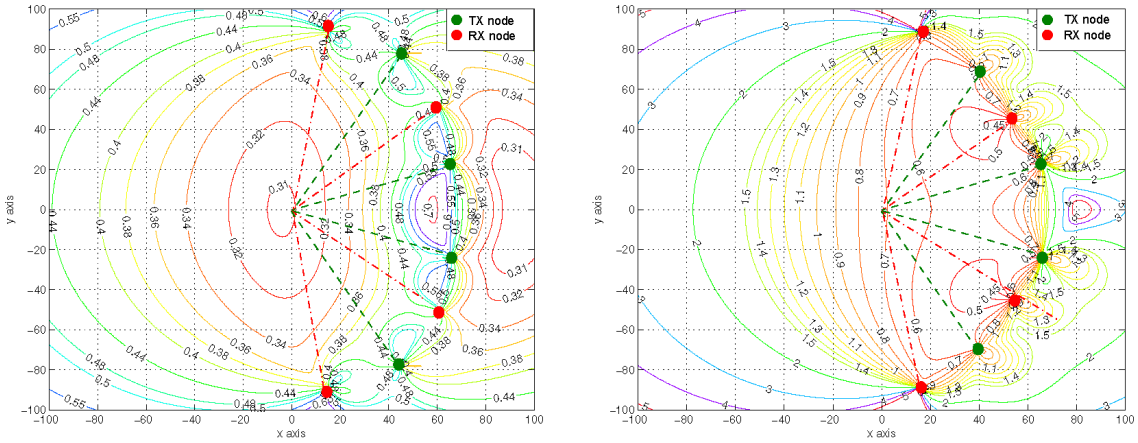

Figure 6: PDOP contour plot with 4 transmitters and 4 receivers asymmetrical placed radar network. Left figure shows the non-coherent case and on the right hand the coherent case. (©IEEE 2009, from [20])

tained for a given radar constellation or for choosing the best node locations to cover a given surveillance area.

5 Conclusion

It has been shown that multistatic radar network performance depends not only on radar parameters, but also on the chosen geometry.
Overall multistatic radar networks have many advantages and can increase the performance of a single radar unit easily. However, these benefits come at the cost of an increased complexity and a high demand on synchronising all nodes in the network.

References

[1] M. WEISS, ”Digital Antenna”, NATO SET-136 Lecture Series ”Multistatic Surveillance and Reconnaissance: Sensor, Signals and Data Fusion”, April 2009

[2] C. BAKER, ”Multistatic Radar Processing and systems”, NATO SET-136 Lecture Series ”Multistatic Surveillance and Reconnaissance: Sensor, Signals and Data Fusion”, April 2009

[3] J. LI AND P. STOICA, "MIMO radar signal processing", John Wiley & Sons, Inc., Hoboken, New Jersey, 2009

[4] NICHOLAS J. WILLIS, "Bistatic Radar", Artech House, Boston, London, 1991

[5] S. HUANG, M. TU, S. YAO, L. MALEKI, "A turnkey optoelectronic oscillator with low acceleration sensitivity", Proceedings of the IEEE/EIA International Frequency Control Symposium and Exhibition, 2000, pp. 269-279

[6] M. WEISS, "Synchronization of bistatic Radar systems", IEEE 2004 International Geoscience and Remote Sensing Symposium, Anchorage, Alaska, USA, pp. 1750-1753

[7] P.M. WOODWARD, "Probability and Information Theory with Applications to Radar", Pergamon, New York, 1953

[8] N. LEVANON, "Radar principles", Wiley, 1998

[9] T. TSAO, M. SLAMANI, P. VARSHNEY, D. WEINER, H. SCHWARZLANDER, S. BOREK, "Ambiguity function for a bistatic radar", IEEE Transactions on Aerospace and Electronic Systems, Vol. 33, No. 3, July 1997, pp. 1041-1051

[10] C. BAKER, "Multistatic radar processing and systems", NATO SET-136 Lecture Series "Multistatic Surveillance and Reconnaissance: Sensor, Signals and Data Fusion", April 2009

[11] H. GODRICH, A.M. HAIMOVICH, R.S. BLUM, "Target localization techniques and tools for MIMO radar", submitted to IEEE Trans. on Information Theory.

[12] F.C. ROBEY, S. COUTTS, D. WEIKLE, J.C. MCHARG, K. CUOMO, "MIMO radar theory and experimental results", in Proc. of 37th ASILOMAR 2004 Conf. on Signals, Systems and Computers, Nov. 2004, pp. 300-304

[13] I. BEKKERMAN, J. TABRIKIAN, "Target detection and localization using MIMO radars and sonars", IEEE Trans. on Sig. Proc., Vol. 54, Oct. 2006, pp. 3873-3883

[14] L. XU, J. LI, P. STOICA, "Adaptive techniques for MIMO radar" in 14th IEEE Workshop on Sensor Array and Multi-channel Processing, Waltham, MA, July 2006.

[15] E. FISHLER, A.M. HAIMOVICH, R.S. BLUM, L. CIMINI, D. CHIZHIK, R. VALENZUELA, "Spatial diversity in radars - models and detection performance", IEEE Trans. on Sig. Proc., Vol. 54, pp. 823-838, March 2006

[16] N. LEHMANN, A.M. HAIMOVICH, R.S. BLUM, L. CIMINI, "MIMO - radar application to moving target detection in homogenous clutter", 14th IEEE Workshop on Sensor Array and Multi-channel Processing, Waltham, MA, July 2006

[17] N. LEHMANN, A.M. HAIMOVICH, R.S. BLUM, L. CIMINI, "High resolution capabilities of MIMO radar", Proc. of 40th ASILOMAR 2006 Conference on Signals, Systems and Computers, Nov. 2006

[18] H. GODRICH, A.M. HAIMOVICH, R.S. BLUM, "Cramer Rao Bound on Target Localization Estimation in MIMO Radar Systems", in Proc. of CISS Conf., March 2008.

[19] S.M. KAY, "Fundementals of Statistical Signal Processing: Estimation Theory", Vol. 1, New Jersey: Parentice Hall PTR, 1st ed., 1993

[20] H. GODRICH, A.M. HAIMOVICH, R.S. BLUM, "Target localization techniques and tools for multiple-input multiple-output radar", IET Radar, Sonar & Navigation, 2009, Vol. 3, Iss. 4, pp. 314-327

[21] R.B. LANGELEY, "Dilution of Precision", GPS World, May 1999, pp. 52-59

[22] H.B. LEE, "A novel procedure for assessing the accuracy of the hyperbolic multilateration systems", IEEE Trans. on Aerospace and Electronic Systems, Vol. 11, Jan. 1975, pp. 2-15

[23] N. LEVANON, "Lowest GDOP in 2-D scenarios", IEE Proc. Radar, Sonar, Navigation, Vol. 147, June 2000, pp. 149-155

[24] R. YARLAGADDA, I. ALI, N. AL-DHAHIR, J. HERSHEY, "GPS GDOP metric", IEE Proc. Radar, Sonar, Navigation, Vol. 147, No. 5, October 2000, pp. 259-264